Nonlinear ultrasonically induced birefringence in gold sols: Frequency-dependent diffusion

H. Daniel Ou-Yang, Richard A. MacPhail,* and Daniel Kivelson
Department of Chemistry, University of California, Los Angeles, California 90024
(Received 13 May 1985)

Ultrasonically induced birefringence has been used to study coupled translational and rotational motions of large (100-nm) nonspherical colloidal gold particles in fluids. The effect is nonlinear in that the induced birefringence is quadratic in the ultrasonic amplitude. A theory is developed to explain the dependence of the observed signal on concentration, viscosity, temperature, particle size, and on the ultrasonic intensity and frequency. This enables us to determine the frequency dependence of the viscous drag on the translational motion of nonspherical Brownian particles.

I. INTRODUCTION

Optical anisotropy may be induced in an initially isotropic liquid consisting of nonspherical molecules by orienting the molecules with ultrasonic waves.[1,2] In this paper we report a study of ultrasonically induced birefringence in gold sols. Our analysis yields information concerning rotational and frequency-dependent translational motions of large nonspherical colloidal particles, as well as the nonlinear coupling of these motions to each other.

Early ultrasonically induced birefringence studies have been reviewed by Hilyard and Jerrard.[3] For neat liquids composed of small nonspherical molecules, the ultrasonically induced birefringence is well described by linear theories in which the molecular orientation couples to the velocity gradient of the ultrasonic wave.[4,5] These theories predict, in accord with observations, a birefringence which is proportional to the ultrasonic frequency, to the solvent viscosity and to the square root of the ultrasonic intensity.[5-7]

In colloidal suspensions of large nonspherical particles, the ultrasonically induced birefringence is very different from that in neat liquids. Oka suggested that in a colloidal suspension of rigid particles the coupling between the ultrasonic wave and particle orientation should be dominated by a sound-pressure mechanism,[8] as in the Rayleigh-Disk problem.[9-12] The predicted induced birefringence is then nonlinear, i.e., proportional to the square of the amplitude (A) of the ultrasonic wave, but independent of the ultrasonic frequency (Ω) and solvent viscosity (η). Few ultrasonically induced birefringence experiments have been carried out to date on colloidal systems. Jerrard's measurements[6] on bentonite suspensions indicated a birefringence which is indeed proportional to the ultrasonic intensity, but one that increases with increasing ultrasonic frequency. Lipeles and Kivelson[5] examined gold sols and concluded that the birefringence had a large component proportional to the ultrasonic intensity, but their data were not sufficiently reliable to provide information on the frequency dependence. We have measured the "nonlinear" birefringence induced in gold sols as a function of ultrasonic intensity and frequency, as well as the viscosity, temperature (T), particle size, and volume fraction (C_v). The gold sols are composed of disks with radii a small compared to both the light and ultrasound wavelengths. Oka's theory successfully explains the dependence upon ultrasound intensity, but fails to account for the observed dependences on ultrasonic frequency, solvent viscosity, and particle size, and it predicts the wrong sign for the birefringence of metallic particles.

We have developed a modified version of Oka's theory in which the viscous drag of the solvent on the translational motion of the suspended particles is incorporated. Comparison of our data with the predictions of this modified theory suggests that the frequency dependence of the translational diffusion is responsible for the observed frequency and viscosity dependence of the induced birefringence. We have explained the observed sign of the birefringence in gold sols by modifying the Peterlin and Stuart theory[13] for the optical anisotropy of an aligned particle.

II. EXPERIMENTAL

Although the measurement of birefringence is conceptually simple, a number of experimental features require special attention. The detection system has to be very sensitive and capable of distinguishing a nonlinear birefringence (proportional to the ultrasonic intensity A^2) from a linear one (proportional to the amplitude A). Since we wish to know the relationship between birefringence and both ultrasonic intensity and frequency, it is necessary to measure the absolute ultrasonic intensity (at each frequency) at the exact region in the sample where the light beam and the ultrasonic wave intersect. Because the ultrasonically induced birefringence from dilute solutions of suspended particles is very small, care must be exercised to reduce parasitic effects, such as the induced birefringence in the solvents or in the optical elements, which may mask the desired signals. Heating and streaming may occur due to absorption of the sound wave. More importantly, the loss of light due to diffraction by sound-induced density waves (Debye-Sears effect) can complicate the analysis of the data, and ultimately limit the sensitivity of the experiment. Experimental details are given in Ref. 14.

A. The gold-sol samples

The gold sols are aqueous solutions of rigid submicrometer gold disks. Since the optical properties of the gold particles are very different from those of the solvent, the induced birefringence is large. The sols were prepared from analytical grade gold chloride ($HAuCl_4 \cdot 3H_2O$) crystals, purchased from Matheson, Coleman, and Bell Manufacturing chemists, according to the procedure of Turkevich *et al.*,[14–16] and were brownish red, transmitting blue light. The sol was concentrated by gradually boiling off the water; however, all samples were quite dilute since prolonged heating or vacuum distillation ended in precipitation. The concentrations of the samples were determined by turbidity measurements.[17] The volume fraction of the suspended gold-disks varied from 0.4×10^{-6} to 1.6×10^{-6} for different samples, corresponding to average distances between particles of 50–80 μm, at least 100 times the particle size. Our systems were indeed dilute.

Estimates of the particle sizes were obtained by assuming that the relaxation of the induced birefringence following an ultrasonic pulse is due to the particle reorientation. For an infinitely thin disk, Perrin[18] showed that under "stick" boundary conditions the orientational relaxation time τ is given by

$$\tau = 16\pi\eta a^3/9k_BT\ , \tag{2.1}$$

where k_B is the Boltzmann constant. Mean particle radii a determined by equating τ to the observed birefringence relaxation were in reasonable agreement with the results from electromicrograph experiments.[5,14] By slightly varying the amount of chlorauric acid used in the gold-disk preparation, we obtained samples with mean gold-disk radii increasing from about 100 to 400 nm. The electromicrograph results suggest that the ratio of disk diameter to thickness is about 10:1.

Our analysis indicated that both the relaxation time τ and the birefringence signal are proportional to a^3. This suggests that our experiments selectively detect the larger particles, so that the particles sampled have relatively narrow size distributions. This conclusion is reinforced by the good one-exponential fit of the transient rise and decay processes as indicated in Figs. 1(a) and 1(b). Though the electromicrograph results indicate reasonable monodispersity, we noted a decrease in the measured τ's with time (see Fig. 2), presumably because the larger particles were settling out of solution.

B. The acousto-optic cell

The cell was composed of three major parts: the ultrasonic transducer chamber, the optical chamber, and the absorption chamber. Temperature was controlled by circulating thermostatted fluid in the brass wall (see Fig. 3).

The transducer chamber was at the bottom to guarantee good contact between the transducer crystal and the sample sitting above it. The ultrasonic transducer was an x-cut quartz crystal with coaxially coated gold-chromium alloy conducting electrodes. The diameter (0.8 cm) of the positive electrode defined the ultrasonic beam.

The laser beam and ultrasonic waves intersect in the optical chamber, which contains approximately 18 ml of

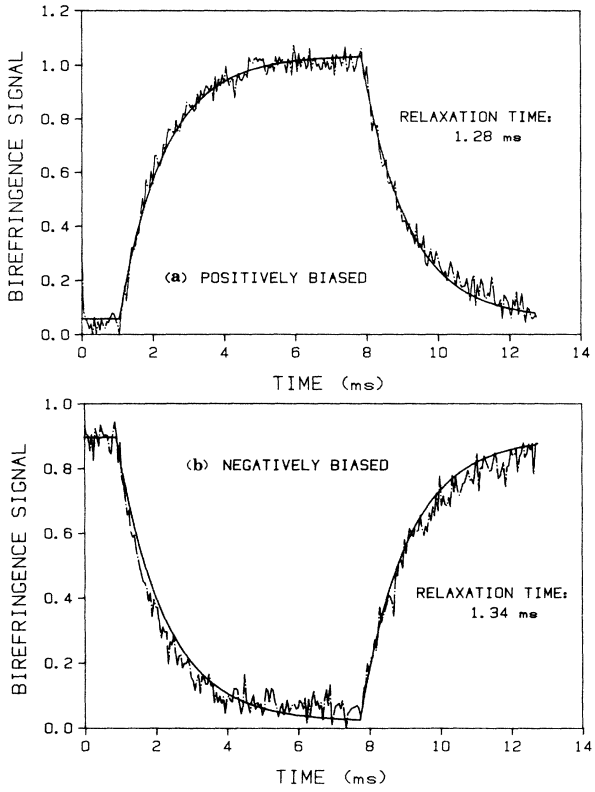

FIG. 1. (a) Representative positively biased birefringence spectrum for a gold sol of particle size 145 nm generated with 7 ms ultrasonic wave pulses. (b) Negatively biased birefringence spectrum for the same sample. The vertical axes are proportional to the birefringence signal. The deviation of the data points from both fitted curves indicates that the particles were not completely monodisperse.

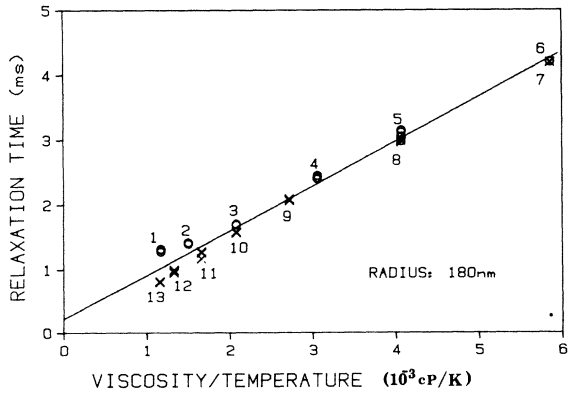

FIG. 2. Relaxation time τ vs η/T. Measurements were made first by cooling and then heating the sample (the numbers indicate the sequence of data points). The large scatter of the data points at low η/T indicates precipitation of some of the larger gold sols during the measurement cycle (about 4 h).

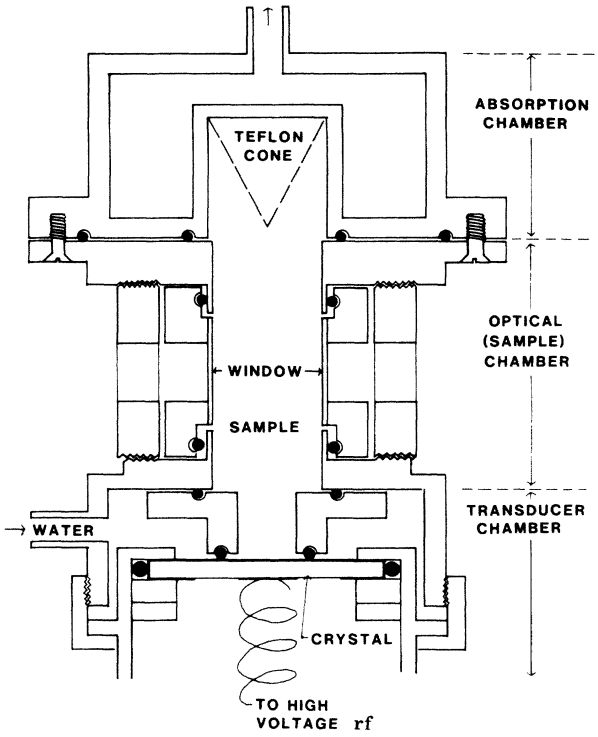

FIG. 3. The acousto-optic cell. The cell is composed of three major parts: the ultrasonic transducer chamber, which houses an x-cut quartz crystal, the optical (sample) chamber, and the absorption chamber. Thermostatted fluid circulates in the brass wall.

sample fluid. Strain birefringence in the windows was minimized by cementing the microscope coverglass windows with flexible silicon rubber. The birefringence induced by ultrasonic waves in the pure solvent and in the optical windows was negligible.

The absorption chamber was at the top and contained a thin porous Teflon cone. The upcoming sound waves were deflected and absorbed in this chamber; therefore, we had "pure" traveling waves. This could be checked by looking for the Debye-Sears diffraction (see later) produced from the reflected ultrasonic pulses. To avoid diffraction of sound waves from bubbles, most air bubbles were excluded, and any left rose above the laser beam.

C. Birefringence measurement

In an ultrasonically induced birefringence experiment one measures the difference, $\Delta n = n_x - n_y$, of the indices of refraction along the direction of ultrasonic wave propagation n_x and perpendicular to it n_y. The incident light (along z) is linearly polarized at an angle of 45° from the x direction, and the analyzer (a Glan-Thompson prism) is set perpendicular to the incident polarization. Since the overall phase retardation due to the birefringence is much less than 1 rad, the intensity of the transmitted light is given by[14,19]

$$I=(I_0-I_b)[(\Delta\psi)^2+2(\Delta\psi)\beta+\beta^2]/4+I_b\ , \tag{2.2}$$

where I_0 and I_b are the light intensities measured in the absence of the ultrasonic wave when the analyzer is parallel and perpendicular, respectively, to the incident laser beam, $\Delta\psi$ and β are the phase retardations caused by the ultrasonically induced birefringence and by all other sources, respectively. The phase retardation $\Delta\psi$ is related to the induced birefringence Δn by

$$\Delta\psi=2\pi(\Delta n\, d)/\lambda_0\ , \tag{2.3}$$

where d is the distance the light travels in traversing the sound wave, and λ_0 the optical wavelength in vacuum.

In our experiment the phase retardation β can be varied by adjusting a quartz waveplate. Since $\Delta\psi$ in our experiment is of the order 10^{-3} rad, we can adjust β such that $2\beta \gg \Delta\psi$, while keeping the total phase retardation $\Delta\psi+\beta$ much less than one radian. We can then neglect $(\Delta\psi)^2$ in Eq. (2.2), and the induced birefringence signal I_s is thus given by

$$I_s=[(\Delta\psi)\beta(I_0-I_b)]/2\ . \tag{2.4}$$

We label this procedure "biased" birefringence detection. If $\Delta\psi$ is linear in the ultrasonic amplitude A, it is oscillatory with the ultrasonic frequency Ω, while if it is "quadratic" in A, it contains a dc term as well as a term that oscillates with frequency 2Ω. In our experiment $\Delta\psi$ is averaged, and only the dc quadratic component is detected. Thus we *experimentally discriminate against any linearly induced birefringence and measure only birefringence from nonlinear effects.*

The ultrasonic waves were pulsed at a low repetition rate (4—30 Hz) to reduce ultrasonic heating and streaming, but the pulse length (5—30 msec) was kept long enough to allow the transient birefringence to reach its maximum. By choosing the bias such that $\beta=(I_b/I_0)^{1/2}$, we maximized the signal-to-noise ratio.[14] The rather "noisy" transient birefringence signals were digitized and sent to a DEC LSI-11/23 laboratory computer for signal averaging (100—2000 scans).

D. Debye-Sears effect and ultrasonic intensity measurement

We need to measure the ultrasonic intensity at the precise volume element in the sample which gives rise to the ultrasonically induced birefringence. This can be done by studying the light diffracted from the "density grating" induced in the sample by the ultrasonic wave (Debye-Sears effect[20–23]). We obtained this information without disturbing the birefringence measurement by utilizing the rejected beam from the analyzer Glan-Thompson prism.

Since the speed of sound V_s is much smaller than that of light, the refractive index variations constitute a stationary diffraction grating. Raman and Nath obtained an expression which relates the light intensity I_m of the mth-order diffraction line to the ultrasonic amplitude A:[23,24]

$$I_m=BJ_m^2(bA)\ , \tag{2.5}$$

where B is a constant, J_m is the Bessel function of order m, b has the form

$$b=\frac{2\pi d}{\lambda_0}\frac{(n_0^2-1)(n_0^2+2)}{6n_0}\left[\frac{2}{\rho_0 V_s^3}\right]^{1/2}. \quad (2.6)$$

ρ_0 is the mass density, and n_0 the refractive index of the medium. In our experiment $d=0.8$ cm, $\lambda_0=4.88\times10^{-5}$ cm, $n_0=1.33$, $V_s=1.5\times10^5$ cm/sec, and $\rho_0=1.0$ g/cm^3; it follows that $b=2.88$ (cm^2/W)$^{1/2}$. By fitting the measured I_1/I_0 to the calculated values of $[J_1(x)/J_0(x)]^2$, we obtained the ultrasonic intensity $A^2/2$. In our experiments the ultrasonic intensity is less than 0.2 W/cm^2. Ultrasonic frequencies used were odd harmonics from 3 to 19 MHz.

III. THEORY

Nonspherical particles or molecules in a liquid can be oriented by ultrasonic waves, and the liquid then becomes birefringent. The birefringence induced in the gold-sol sample is proportional to the mean orientation Q, the optical anisotropy ΔG, and the volume fraction C_v of the particles:[3,14]

$$\Delta n=(2\pi/n_0)(\Delta G)QC_v . \quad (3.1)$$

In isotropic solvents, ΔG is a function of both the shape and dielectric properties of the suspended particles. By an extension of the theory of Peterlin and Stuart,[13] we have shown that the complex optical anisotropy for a spheroid[14] is

$$\Delta G=\frac{(\epsilon-\epsilon_0)^2(N_1-N_3)}{[4\pi\epsilon_0+(\epsilon-\epsilon_0)N_1][4\pi\epsilon_0+(\epsilon-\epsilon_0)N_3]}, \quad (3.2)$$

where ϵ and ϵ_0 are the dielectric permittivities of the suspended particle and the solvent, respectively. The N's, are shape factors along the principal axes of the spheroid for which $N_1=N_2$, and obey the sum rule

$$N_1+N_2+N_3=4\pi . \quad (3.3)$$

For an oblate spheroid,

$$N_3=4\pi(1+\alpha^2)(1-\alpha\cot^{-1}\alpha) \quad (3.4)$$

with $\alpha=c/(a^2-c^2)^{1/2}$, where a and c are the semimajor and semiminor axes of the oblate spheroid, respectively. We shall assume that ΔG for a disk is similar to that for an oblate spheroid.

A. Theory of Oka

Oka assumed that because of the radiation pressure resulting from the passage of ultrasonic waves, large disk-like colloidal particles (with radius much smaller than the ultrasonic wavelength) are subjected to a turning torque that tends to align the particle with the disk axis along the direction of the ultrasonic beam.[9] This theory is closely related to the Rayleigh-Disk problem,[9-12] and is a consequence of the Bernoulli effect.[14] Since the radiation pressure is a second-order nonlinear effect, the torque, and thus the resulting potential energy have a component at twice the ultrasonic frequency Ω as well as a dc component;[3,14] Oka focused on the latter.

Oka neglected all interactions among colloidal particles, a reasonable assumption in dilute solutions, and also assumed that the suspended particles were monodisperse, rigid thin disks. He obtained the distribution of particle orientations for particles subjected to a torque $\mathbf{M}$:[10,12]

$$|\mathbf{M}|=-(1/3)\rho_0 a^3|\mathbf{V}_r|^2\sin2\theta \quad (3.5)$$

where a is the disk radius, ρ_0 the density of the solvent, $\mathbf{V}_r$ the velocity of the fluid relative to the disk, and θ the angle between the normal to the disk and the direction of sound. The negative sign indicates that the torque tends to diminish θ. If the ultrasonic perturbation is weak, such that its energy is small compared with the thermal energy k_BT, then the mean orientation of the particles is given approximately as[3]

$$Q=\tfrac{2}{45}(\rho_0 a^3|\mathbf{V}_r|^2/k_BT) . \quad (3.6)$$

The relative velocity $\mathbf{V}_r$ can be related to the fluid velocity $\mathbf{v}$ by

$$\mathbf{V}_r=f\mathbf{v} , \quad (3.7)$$

where

$$|\mathbf{v}|=(1/\rho_0 V_s)^{1/2}A \quad (3.8)$$

and A is the ultrasonic amplitude. For a disk in an ideal fluid, one without viscosity, it is found[12] that

$$f=(\rho-\rho_0)/[\rho+\rho_0(40/3\pi)] , \quad (3.9)$$

where ρ is the density of the particle, and ρ_0 the density of the fluid. For low ultrasonic intensity, it then follows from Eqs. (3.1) and (3.7)–(3.9) that

$$\Delta n=(4\pi a^3/45k_BTV_s)(\Delta G/n_0)C_v f^2A^2 . \quad (3.10)$$

Oka made use of Peterlin and Stuart's[13] expression for ΔG, which is that given in Eq. (3.2) but with $\epsilon=n^2$ and $\epsilon_0=n_0^2$; for an oblate spheroid this leads to a negative ΔG, and therefore a negative birefringence. However, for conducting particles, both ϵ and ΔG are complex and the real part of ΔG may be positive,[14] which leads to a positive birefringence, as observed for our gold sols. The imaginary part of ΔG corresponds to dichroism and will be discussed later. Comparisons between the predictions of Oka's theory and the experimental data are given in Table I.

B. Modifications of Oka's theory

In Oka's theory the torque exerted on the disk is obtained by solving Euler's equation in a spheroidal coordinate system subject to appropriate boundary conditions.[10-12] Euler's equation holds when the Reynolds number of the fluid system, $R=v\rho_0 a/\eta$, is much larger than 1, i.e., for ideal fluids. But in our experiments the translational Reynolds numbers are of the order 10^{-3}, and the effects of fluid viscosity cannot be ignored. For this case, one could obtain the torque $\mathbf{M}$ on the particle by

TABLE I. Comparison of Oka's theory with experimental data.

	Theory	Experimental data			
	Oka	Petralia (Ref. 25)	Jerrard[a] (Ref. 6)	Lipeles (Refs. 5,14)	This work
Sols		V_2O_5	Bentonite	Gold	Gold
Shape	disk	needle	plate	disk	disk
A dependence[b]	A^2	A^2	A^2	A^2	A^2
Sign of Δn	$-$[c]	$+$[c]	$-$[c]?	?[d]	$+$[d]
Ω dependence	none	?	yes	yes	yes
η dependence	none	yes	?	yes	yes
$\Delta n/a^3$ as function of a	no	?	?	?	yes

[a]Although Jerrard did not report the sign of the birefringence induced in bentonite sols, his discussion suggests a negative sign.
[b]A, acoustic amplitude; Δn, birefringence; Ω, acoustic frequency; η, solvent viscosity; a, particle size.
[c]Nonconducting.
[d]Conducting.

solving the full Navier-Stokes equation, but this would be a difficult task because of the coupling between the rotational and the translational motions of the particle.

Fortunately, the problem can be greatly simplified because the time scales of the particle's rotational and translational motions in the ultrasonic wave are so different; in our studies the period of the oscillatory translational motion is of order 10^{-7} sec, whereas for the rotational motion it is of order 10^{-3} sec. During one cycle of the ultrasonic wave the particle hardly rotates, and one can make an "adiabatic" approximation[14] for the particle's orientation. To do so, one first calculates the translational velocity of the particles in an ultrasonic wave for a fixed orientation and then calculates the torque for each orientation by treating the particle as a Rayleigh-Disk. In this approach the torque on the particle is still given by Eq. (3.5) and the velocity $\mathbf{V}_r$ by Eq. (3.7), but the function f in Eq. (3.9) is replaced by one that includes the viscous effects on the translational motion of the particles. However, although the translational motion of a Brownian sphere in a viscous fluid is well known,[25,26] for a nonspherical particle at an arbitrary orientation it is more complicated, and further approximation is necessary. The adiabatic approximation is valid when translational (or ultrasonic) frequencies Ω are much higher than the reorientational frequencies $1/\tau$ of the particles, which is the case in our experiments.

C. Translation of a Brownian sphere in ultrasonic waves

In studying the translational motion, we first consider a Brownian sphere immersed in an oscillating fluid. We assume that the wavelength of the ultrasound is much larger than the dimension a of the sphere, i.e., $\Omega \ll V_s/a$, where V_s is the speed of sound. We let $\mathbf{u}(x)\exp(-i\Omega t)$ be the velocity of the sphere and $\mathbf{v}(x)\exp(-i\Omega t)$ the velocity of the liquid flow far from the sphere, where both $\mathbf{v}(x,t)$ and $\mathbf{u}(x,t)$ are referred to the laboratory coordinate frame.

There are two forces acting on the sphere. The first is a drag force due to the relative motion of the fluid with respect to the sphere; this force (stick boundary conditions), as given by Masters and Madden[27] in the frequency domain, is

$$\mathbf{F}_1=\zeta\Phi[R_L](\mathbf{v}-\mathbf{u}) , \tag{3.11}$$

where ζ is the Stokes drag coefficient, and

$$\Phi[R_L]=(1+\sqrt{R_L})-i(\sqrt{R_L}+\gamma R_L) . \tag{3.12}$$

For a sphere $\zeta=6\pi\eta a$, $\gamma=\frac{2}{9}$. The "librational Reynolds number"[28] R_L is defined as

$$R_L=\Omega/\Gamma \tag{3.13}$$

and the frequency of viscous translational response Γ is given by

$$\Gamma=2\eta/a^2\rho_0 . \tag{3.14}$$

The equivalent result in the time domain is given by Landau and Lifshitz.[26] The $\sqrt{R_L}$ terms in Eq. (3.12) come from the interplay between inertial and viscous effects and are closely related to the "long-time tail" behavior.[27]

The second contribution to the force is, in the frequency domain, given by

$$\mathbf{F}_2=-i\Omega\rho_0\phi\mathbf{v} , \tag{3.15}$$

where ϕ is the molecular volume, which for a sphere is

$$\phi=(4\pi/3)a^3 . \tag{3.16}$$

This is the force that would be exerted on the sphere if it were replaced by fluid with the same volume, in which case it would move like the rest of the flowing liquid.

The total force, $\mathbf{F}_1+\mathbf{F}_2$, on the sphere is equal to $\rho\phi d\mathbf{u}/dt$, which is $-i\Omega\rho\phi\mathbf{u}$ in the frequency domain; combining this equality with the expressions for $\mathbf{F}_1$ and $\mathbf{F}_2$ given above and the definition of f in Eq. (3.7), we find

$$f=\frac{\rho-\rho_0}{\rho+i(\zeta/\phi\Omega)\Phi[R_L]} . \tag{3.17}$$

Since f is complex, the translational motion of the particle with respect to the fluid has both in-phase and out-of-phase components.

D. Translation of a thin disk

The coefficients of zero-frequency Stokes drag are $16\eta a$ and $32\eta a/3$ for a disk moving in the direction of its axis or perpendicularly to it,[29] respectively; for a sphere it is $6\pi\eta a$. Even for the special motion of a disk along a symmetry axis, for which there is no coupling between translations and rotations, we do not know how to evaluate the frequency-dependent drag coefficient, but we assume that it is given by the appropriate zero-frequency coefficient multiplied by the same frequency factor $\Phi[R_L]$ applicable to spheres. Furthermore, since the coefficient of zero-frequency drag differs by less than a factor of 2 for motions along the principal axes, we assume that the effective frequency-dependent drag coefficient for a disk is reasonably well represented by that for motion along its unique axis. For a disk (with diameter to thickness ratio of 10:1) moving along its unique axis, the relative velocity $\mathbf{V}_r$ is then given by Eqs. (3.7), (3.12), and (3.17), with the factor f specified by

$$\zeta = 16\eta a \ , \tag{3.18}$$

$$\phi = \pi a^3/5 \ , \tag{3.19}$$

and

$$\gamma = \tfrac{1}{3} \ . \tag{3.20}$$

The γ for a disk differs from that of a sphere because the "induced mass" is different;[26,29] we obtained this value of γ by requiring that Eq. (3.17) reduces to Eq. (3.9) for a disk in an ideal fluid.

E. Frequency dependence of the induced birefringence

The birefringence of a disk in viscous fluid is given by Eqs. (3.10) and (3.17)–(3.20). Note that the frequency dependence of the birefringence comes from the disk's translational motion, through Eq. (3.7). Since the birefringence is proportional to $|\mathbf{V}_r|^2$ and thus to $|f|^2$, we examine the frequency dependence of f. We shall look at the translational motion in a few limiting cases, which are distinguished by the relative values of the frequencies of the acoustic field Ω, viscous translational relaxation Γ, and reorientational relaxation $1/\tau$ of the particle. Note that the acoustic frequency must satisfy the inequalities $V_s/a \gg \Omega \gg 1/\tau$; the first inequality ensures that the acoustic wavelength is much larger than the particle size, the second one is necessary for the adiabatic approximation to hold.

(1) In the high-Ω limit, where $R_L \gg 1$, one obtains the ideal fluid result given in Eq. (3.9). In this case the birefringence is independent of Ω, as indicated by Oka; the particle cannot respond to the ultrasonic oscillation and is, therefore, "pinned," which enables a large torque to develop.

(2) In the low-Ω limit, where $1/\tau\Gamma \ll R_L \ll 1$, one obtains

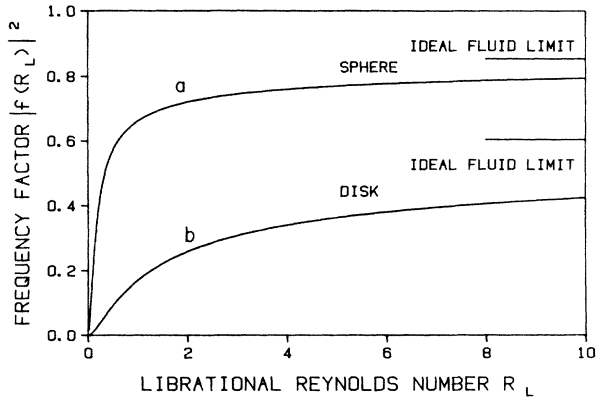

FIG. 4. Frequency factor $|f|^2$ as a function of the librational Reynolds number R_L for a a sphere and b a spheroid of major to minor axis ratio 10:1; ρ/ρ_0 is 19.3.

$$f = -i(\pi/80)a^2(\Omega/\eta)(\rho-\rho_0) \ , \tag{3.21}$$

which is linear in ultrasonic frequency; this leads to a birefringence Δn which is proportional to Ω^2. The particle librates with the ultrasonic wave, thereby diminishing the torque. A recent theory due to Ronis[30] also predicts the Ω^2 dependence, but it is applicable only in the very low frequency regime, $\Omega\tau \ll 1$, well below the range of our experiments. For our experiments $\Omega\tau \gg 1$, and $0.1 \leq R_L \leq 10$.

In Fig. 4 we have plotted $|f|^2$ against the librational Reynolds number R_L for both a disk and a sphere. The figure shows that at very high librational Reynolds number both curves approach that for an ideal fluid asymptotically, but slowly. At low librational Reynolds number the relative velocity, $\mathbf{V}_r = f\mathbf{v}$, vanishes. At large R_L (large particle, low viscosity, or high frequency) inertial effects dominate, as in the case of an ideal fluid. At low R_L the viscous drag predominates and the particles move along with the solvent, as in the case of molecules in neat liquids. Thus one would expect the nonlinear effects to dominate at high Reynolds number R_L, while at sufficiently low Reynolds number these effects diminish so much that the linear effects dominate. One should note that the amplitude of the relative velocity $\mathbf{V}_r$ is dependent upon the density ratio (ρ/ρ_0); in fact, one would not expect much relative translational motion for particles with density close to that of the solvent. For gold sols, $(\rho/\rho_0) = 19.3$,[31] in which case $|f|^2$ is large, and the nonlinear effect is relatively easy to observe.

IV. DATA ANALYSIS AND RESULTS

The ultrasonically induced birefringence of gold sols was studied as a function of ultrasonic intensity, frequency, viscosity (temperature), gold-sol concentration, and particle size. In addition, the sign and relaxation of the birefringence were examined. The results of our observations are as follows.

A. Induced birefringence

1. Sign of the induced birefringence

Equation (2.3) shows that the induced birefringence signal is proportional to $\Delta\psi\beta$. Since we could vary the sign of the bias β, we could determine the sign of the induced birefringence. Two birefringence spectra, one with a positive and one with a negative bias, respectively, are illustrated in Figs. 1(a) and 1(b). For all the gold sols examined we found the birefringence to be "positive," which is consistent with our optical anisotropy calculation for gold disks and the prediction that the disks are aligned with the unique axis along the direction of sound-wave propagation.

2. Relaxation time and particle sizes

Both rise and decay transients of the induced birefringence were fitted to a single exponential. The analysis of these transients was discussed in Sec. II.

3. Ultrasonic intensity dependence

The birefringence was measured at fixed ultrasonic frequency Ω as a function of ultrasonic intensity A^2. The straight lines in Fig. 5 indicate that the induced birefringence is proportional to the ultrasonic intensity, a nonlinear effect, in agreement with early experiments and the prediction of Eq. (3.10).

4. Ultrasonic frequency dependence

The induced birefringence was measured at different frequencies (Ω: 3—19 MHz) at a fixed ultrasonic intensity of 0.1 W/cm^2. (This is not equivalent to fixed voltage on the transducer.) The same experiments were repeated on samples with different particle sizes. See Fig. 6.

5. Particle size dependence

The radii of the disks were varied from 100 to 400 nm. For each sample the induced birefringence increases monotonically with frequency, but the functional dependence upon frequency is different for each sample. See Fig. 6.

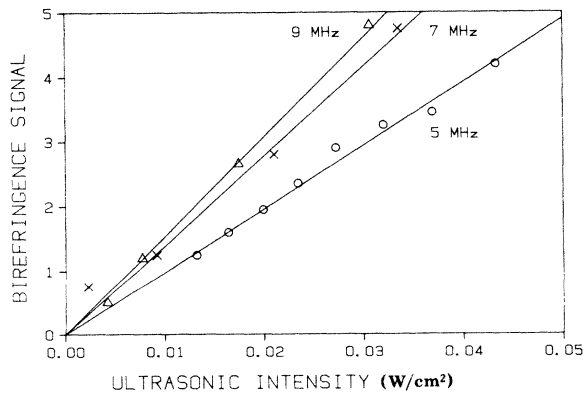

FIG. 5. Induced birefringence vs ultrasonic intensity for frequencies of 5, 7, and 9 MHz, respectively. The straight lines show that the birefringence is nonlinear in acoustic amplitude. The different slopes indicate that this effect is frequency dependent.

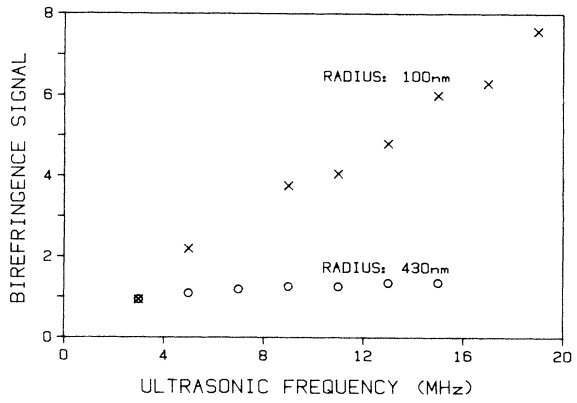

FIG. 6. Ultrasonic frequency dependence of the induced birefringence in gold-sol samples of different particle size; here the birefringence is plotted against the ultrasonic frequency at a constant ultrasonic intensity. The graphs show that the frequency dependence of the birefringence varies with particle's size.

6. Viscosity dependence

The viscosity of the gold sols was varied from 1.6 cp to 0.4 cp (Ref. 31) by changing the temperature of the sample (277—348 K). Because the solutions are dilute, the viscosity of the solution was assumed to be that of pure water. Figure 2 shows that the relaxation time of the transient birefringence signal is proportional to η/T, as predicted by Eq. (2.1); this supports the view that the relaxation of birefringence is chiefly due to the reorientation of particles. In order to compensate for the $1/k_BT$ factor associated with thermal randomization, see Eq. (3.6), in Fig. 7 we plotted the temperature times the birefringence against 1/viscosity; the plot shows that the induced birefringence decreases with increasing viscosity.

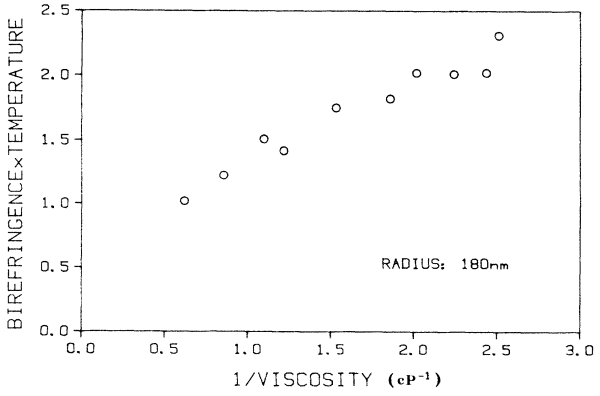

FIG. 7. ΔnT vs $1/\eta$.

7. *Birefringence versus librational Reynolds number*

Since the viscosities and disk radii are known, we can determine the characteristic frequency $\Gamma=2\eta/a^2\rho_0$ for each sample. We actually do not measure Δn but the quantity S, where

$$S=\mathscr{A}[(I_0-I_b)\beta\Delta\psi] . \tag{4.1}$$

$\mathscr{A}$ is an instrumental factor; from Eq. (2.3) we see that S is proportional to Δn. We can write

$$S=K\,|f(R_L)|^2 , \tag{4.2}$$

where

$$K=\frac{8\pi^2 dA^2}{45\lambda_0 k_B T n_0 V_s}[\mathscr{A}(I_0-I_b)a^3\beta C_v\Delta G] \tag{4.3}$$

and $f(R_L)$ is given by Eq. (3.17). K cannot be accurately evaluated because many of the factors in Eq. (4.3), particularly that in square brackets, can only be estimated. Of greater concern is the fact that the quantities in square brackets may vary from sample to sample. We have fitted the proportionality constant K for each sample by means of a least-square fit. The K's are, of course, different for each sample. In Fig. 8, we have plotted the "experimental" S/K values versus the librational Reynolds number R_L. All the data points fall close to the "theoretical" curve for disks given in Fig. 4 and Fig. 8.

Δn can be estimated from Eq. (3.10) but the estimates of ΔG and C_v are imprecise. On the other hand, we can estimate Δn by means of Eqs. (4.1) and (2.3), but the estimates of β, I_0-I_b, and particularly the instrumental factor $\mathscr{A}$ are even more uncertain. The estimate of Δn from Eq. (3.10) is an order of magnitude larger than that obtained by means of Eqs. (4.1) and (2.3). Typically in our experiments the birefringence was in the range 10^{-7}–10^{-8}.

B. Other forms of optical anisotropy

Dichroism or other types of ORD (optical rotatory dispersion) can be distinguished from birefringence by the fact that the former rotates linearly polarized light, and the latter converts linearly polarized light into elliptically polarized light. Dichroism is related to the imaginary part of the ΔG in Eq. (3.2). We found the induced dichroism and other ORD's to be negligible; theoretical estimates of the dichroism for gold disks suggest that it should be at least 2 orders of magnitude weaker than the birefringence for visible light.[14]

Though gold sols scatter visible light very strongly, the light depolarization due to multiple light scattering detected by our pulsed acoustic system should be much smaller than the birefringence signal in our measurements (by at least 4 orders of magnitude).[14]

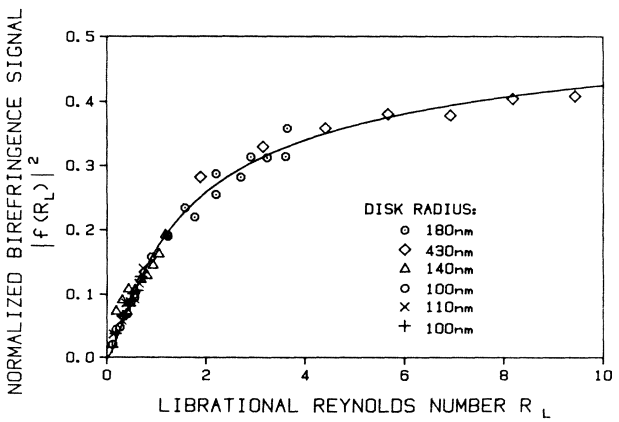

FIG. 8. S/K vs R_L. The data here include those from Figs. 5 and 7. They have been scaled and fit to the theoretical curve *b* in Fig. 4.

V. SUMMARY

We have studied the birefringence is aqueous solutions of dilute gold disks with radii ranging from about 100 to 400 nm and a thickness to diameter ratio of 1:10. The ultrasonic frequency was varied from 3 to 19 MHz, and the dependence of the birefringence on viscosity and particle size were examined. Though the sol solutions were not monodisperse, our measurements on a given sample were sensitive to disks with a relatively narrow range of radii.

A. Instrumental

Our acousto-optic system enables us to measure simultaneously the birefringence signal and the absolute ultrasonic intensity at the point where the laser light interacts with the traveling acoustic wave. The "biased" birefringence detection system discriminates against linearly induced birefringence in favor of nonlinear signals, and allows us to tell the sign of the birefringence and to maximize the signal-to-noise ratio. The pulse mode of operation enabled us to check that none of the birefringence was induced by a reflected wave.

B. Experimental results

We find that the ultrasonically induced birefringence of gold-sol particles in aqueous solution (1) has a positive sign, (2) has a relaxation time which is linearly proportional to η/T, and is consistent with the rotational relaxation time of the disk particles, (3) is proportional to the ultrasonic intensity A^2, (4) increases monotonically with disk size a, (5) varies with ultrasonic frequency Ω —from a quadratic dependence at low frequencies to no dependence at high frequencies, (6) decreases with increasing viscosity at a fixed temperature, (7) is described by our theory [Eqs. (3.10) and (3.17)].

C. Theory

1. *Optical properties*

We have generalized the formula of Peterlin and Stuart for the optical anisotropy of an oriented anisometric colloidal particle to include conducting particles,[14] see Eq. (3.2). This explains the observed positive birefringence in gold sols.

2. *Hydrodynamic properties*

We have developed a radiation pressure theory for the birefringence induced by traveling ultrasonic waves, which includes viscous effects on the translational motion of the suspended particles. The birefringence due to radiation pressure is nonlinear in that it is quadratic in the amplitude of the ultrasonic wave. Our theory shows that the frequency dependence of the translational motion, or equivalently of the diffusion constant of the particles, is responsible for the observed frequency dependence in the birefringence. According to this theory, at very high librational Reynolds number, the colloidal particles behave like Rayleigh disks, and Oka's theory is recaptured; at low librational Reynolds number, viscous effects dominate and damp out the birefringence due to radiation pressure. Consequently, at low librational Reynolds number the magnitude of the nonlinear birefringence diminishes, eventually crossing over to the regime where fluid velocity gradients dominate and the birefringence is linear in acoustic amplitude, as is the case for small molecules in neat liquids. We note that while the diminution of the nonlinear effect at low Reynolds numbers was observed in this experiment, the crossover to the linear behavior was *not observed* because our pulsed, biased detection system specifically discriminates against the linear effect (see Sec. II C). This study gives *direct* evidence for the presence of a frequency-dependent Stokes drag on nonspherical Brownian particles.

ACKNOWLEDGMENTS

We are grateful to the National Science Foundation for its generous support. We wish to thank Professor R. Orbach, Professor P. Chaikin, and Professor D. Ronis and Dr. G. Maret for their helpful comments concerning this work. We also thank B. Klemme for developing the computer programs.

---

*Present address: Department of Chemistry, Duke University, Durham, NC 27706.

[1]R. Lucas, C. R. Acad. Sci. **206**, 827 (1938).
[2]F. J. Burger and K. Söllner, Trans. Faraday Soc. **32**, 1598 (1936).
[3]N. C. Hilyard and H. G. Jerrard, J. Appl. Phys. **33**, 3470 (1962).
[4]R. Lipeles and D. Kivelson, J. Chem. Phys. **67**, 4564 (1977).
[5]R. Lipeles and D. Kivelson, J. Chem. Phys. **72**, 6199 (1980).
[6]H. G. Jerrard, Ultrasonics **2**, 74 (1964).
[7]P. Martinoty and M. Bader, J. Phys. (Paris) **42**, 1097 (1981).
[8]S. Oka, Z. Phys. **116**, 632 (1940).
[9]B. W. S. Rayleigh, *Theory of Sound,* 2nd ed. (Dover, New York, 1945), p. 43.
[10]L. V. King, Proc. R. Soc. London Ser. A **153**, 1 (1935); **153**, 17 (1935).
[11]M. Kotani, Proc. Phys. Math. Soc. Jpn. **15**, 30 (1933).
[12]A. B. Wood, Proc. Phys. Soc. London **47**, 779 (1935).
[13]A. Peterlin and H. A. Stuart, Z. Phys. **112**, 1 (1939).
[14]H. D. Ou-Yang, Ph.D thesis, UCLA, 1985.
[15]R. Lipeles, Ph.D. thesis, UCLA, 1978.
[16]J. Turkevich, P. G. Stevenson, and J. Hillier, Discuss. Faraday Soc. **11**, 55 (1951).
[17]J. D. Jackson, *Classical Electrodynamics,* 2nd ed. (Wiley, New York, 1975), p. 423.
[18]F. Perrin, J. Phys. Radium **5**, 497 (1934).
[19]G. R. Fowles, *Introduction to Modern Optics,* 2nd ed. (Holt, Rinehart, and Winston, New York, 1975).
[20]M. Born and E. Wolf, *Principles of Optics,* 6th ed. (Pergamon, Oxford, 1983), Chap. XII.
[21]M. V. Berry, *The Diffraction of Light by Ultrasound* (Academic, New York, 1966).
[22]P. Debye and F. W. Sears, Proc. Nat. Acad. Sci. U.S.A. **18**, 409 (1932).
[23]C. V. Raman and N. S. N. Nath, Proc. Indian Acad. Sci. Sect. A **2**, 406 (1935); **2**, 413 (1935); **3**, 75 (1936); **3**, 119 (1936).
[24]T. F. Hueter and R. H. Bolt, *Sonics* (Wiley, New York, 1955).
[25]S. Petralia, Nuovo Cimento **17**, 378 (1940).
[26]L. D. Landau and E. M. Lifshitz, *Fluid Mechanics* (Pergamon, Oxford, 1982), pp. 31–36 and 95–96.
[27]A. J. Masters and P. A. Madden, J. Chem. Phys. **74**, 2450 (1981).
[28]J. Happel and H. Brenner, *Low Reynolds Number Hydrodynamics* (Prentice-Hall, Englewood Cliffs, N.J., 1965).
[29]H. Lamb, *Hydrodynamics,* 6th ed. (Cambridge University Press, Cambridge, England, 1932).
[30]D. Ronis, Physica (Utrecht) **120A**, 369 (1982).
[31]*CRC Handbook of Chemistry and Physics,* 52nd ed. (Chemical Rubber, Cleveland, 1971).